CLASSIFICATION OF ULTRASONIC WELD INSPECTION DATA USING PRINCIPAL COMPONENT ANALYSIS

Sangmin Bae, Lalita Udpa, and Satish Udpa
Department of Electrical and Computer Engineering
Iowa State University
Ames, IA 50011

Tom Taylor
Electric Power Research Institute
1300 W. Harris Blvd.
Charlotte, NC 28262

INTRODUCTION

Recent inservice inspection experience, round robin tests of ultrasonic inspection reliability [1] and calculations of flaw detection reliability necessary for specific nuclear power plant applications have consistently shown the need to improve the reliability of ultrasonic inspection. The need to improve ultrasonic inspection reliability is further emphasized when one reviews the pass rates for performance demonstrations specified by ASME Section XI Appendix VIII.

Several years ago EPRI initiated research to explore the feasibility of using neural networks technology to improve the reliability of ultrasonic inspection by reducing the influence of human variability on data analysis. Characterization and classification of ultrasonic inspection data by human operators is tedious and subject to extreme variability [2]. This paper presents a new defect classification method intended to reduce the human variability in ultrasonic weld inspection. The classification technique is based upon principal component analysis (PCA). Several techniques for automatic classification have been proposed [3, 4, 5]. PCA, the oldest and best known technique in multivariate analysis [6, 7], has been used for data compression [8] and acoustic signal classification [9]. The technique is applied in this work to provide features in a reduced dimensional feature space for ultrasonic signals.

ULTRASONIC WELD INSPECTION SIGNALS

The ultrasonic inspection of a pipe in a nuclear power plant is performed by scanning an area of the pipe surface near a weld, to find cracks in the pipe wall as shown in Figure 1.

Review of Progress in Quantitative Nondestructive Evaluation, Vol 16
Edited by D.O Thompson and D.E. Chimenti, Plenum Press, New York, 1997

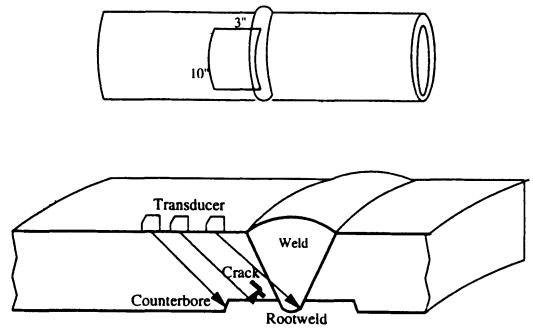

Figure 1: Ultrasonic weld inspection for nuclear power plant pipes: areas around welding are scanned.

A C-scan ultrasonic image is obtained from the maximum amplitude of each A-scan acquired in the scanning area. Examples of C-scan images from a 10"×3" surface area are shown in Figure 2. It is seen that the images contain indications of three classes: rootweld, counterbore and crack. The two areas 'A' in the center represent crack signals. Two horizontal strips 'B' shown at axial position 1" and 2" represent counterbore signals from bottom of the pipe wall. The more strips 'C' at 0.5" axial position represents ultrasonic reflection from the rootweld.

Typical a-scan signals due to counterbores, rootwelds and cracks are shown in Figure 3. The signals are taken from neighboring positions on the scanning area. It is observed that an A-scan signal by itself is not easily discriminated because of the similarity in the shape of waveforms. However, the counterbore is a geometrically machined surface whereas cracks contain randomly oriented facets and welds are inherently heterogeneous. Consequently when a collection of A-scans in a

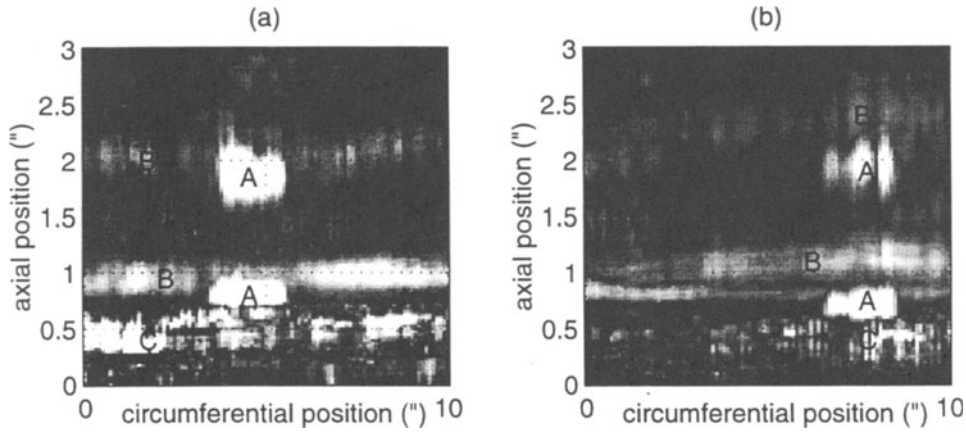

Figure 2: C-scan images, image (a) and image (b) with crack ('A'), counterbore ('B') and rootweld ('C') areas.

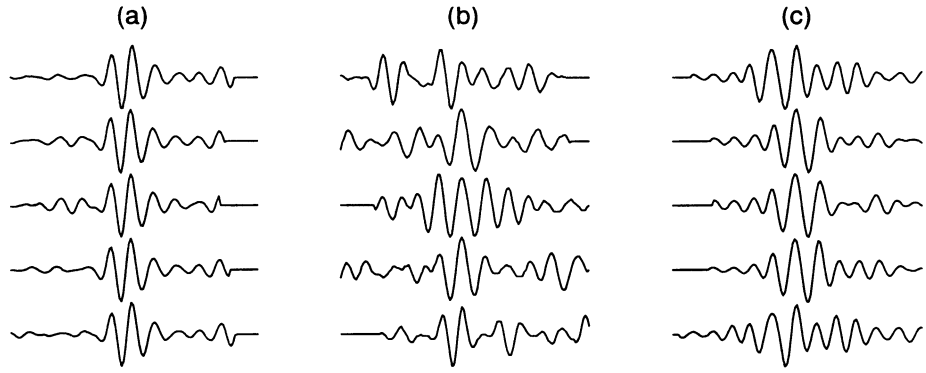

Figure 3: Comparison of typical A-scan signals from (a) counterbores, (b) rootwelds and (c) cracks.

neighborhood are examined, it is observed that reflections from a counterbore show consistency of shape, while rootweld and crack signals exhibit relatively larger amount of variation. This paper describe a technique that is based on the variation of A-scans in a neighborhood, for interpreting the data in a C-scan image.

In the next section, two features representing the signal variation are introduced. The features extract variance and covariance information between signal vectors using an orthogonal projection method called principal component analysis.

PRINCIPAL COMPONENT ANALYSIS

Let each A-scan signal $\vec{x}$ be a vector of p random variables.

$$\vec{x} = [x_1\, x_2\, ,,\, x_p]^T \tag{1}$$

The covariance matrix, C, of $\vec{x}$ is defined as

$$C = E[\vec{x}\vec{x}^T] = \begin{bmatrix} E[x_1x_1] & E[x_1x_2] & ... & E[x_1x_p] \\ E[x_2x_1] & E[x_2x_2] & ... & E[x_2x_p] \\ & & ... & \\ E[x_px_1] & E[x_px_2] & ... & E[x_px_p] \end{bmatrix} \tag{2}$$

with its eigenvalues, $\lambda_1 > \lambda_2 > ... > \lambda_p$, in descending order, and corresponding eigenvectors, $\vec{e}_1, \vec{e}_2, ...\vec{e}_p$. We can define a matrix consisting of the eigenvectors as

$$V = [\vec{e}_1\ \vec{e}_2\ ...\ \vec{e}_p] \tag{3}$$

The principal components of $\vec{x}$ are calculated as

$$\vec{u}^T = \vec{x}^T V = \vec{x}^T[\vec{e}_1\, \vec{e}_2 ... \vec{e}_p] \tag{4}$$

The first eigenvector $\vec{e}_1$ represents the direction of the maximum variance in $\vec{x}$ and the second eigenvector $\vec{e}_2$, orthogonal to $\vec{e}_1$, represents the second largest variance

direction, and so on. The projection $\vec{u}_k^T = \vec{x}^T \vec{e}_k$, where $k = 1, 2, .., p$, provides the measure of variance of the p random variables as well as the structure of covariance between p variables. It is known that the projection

$$\vec{u}^T = \vec{x}^T [\vec{e}_1 \ \vec{e}_2 \ ... \ \vec{e}_q] \tag{5}$$

using only $q(\ll p)$ eigenvectors corresponding to q highest eigenvalues preserves most of the information given by the variance and covariances [6]. Consequently, the dimension of the data vector to be analyzed and processing complexity can be greatly reduced.

For the classification of the ultrasonic signals representing three classes, counterbore, rootweld, crack, two kinds of feature based on principal component analysis were investigated. These features are described below. found to be useful.

Feature A: Signal Variance

Feature 'A', based on signal variance, uses the eigenvalues of the covariance matrix rather than eigenvector. First, an estimate of covariance matrix, $\hat{C}$ is calculated from a set of N neighboring ultrasonic signals, $\vec{x}^n, n = 1, 2, ..., N$, of length p as,

$$\hat{C} = \begin{bmatrix} \hat{E}[x_1x_1] & \hat{E}[x_1x_2] & ... & \hat{E}[x_1x_p] \\ \hat{E}[x_2x_1] & \hat{E}[x_2x_2] & ... & \hat{E}[x_2x_p] \\ & & ... & \\ \hat{E}[x_px_1] & \hat{E}[x_px_2] & ... & \hat{E}[x_px_p] \end{bmatrix} \tag{6}$$

where the estimate of $\hat{E}[x_ix_j]$, $i, j = 1, 2, ..., p$, is defined as

$$\hat{E}[x_ix_j] = \frac{1}{N}\sum_{n=1}^{N}(x_i^n - \frac{1}{N}\sum_{n=1}^{N} x_i^n)(x_j^n - \frac{1}{N}\sum_{n=1}^{N} x_j^n) \quad i, j = 1, 2, ..., p \tag{7}$$

The eigenvalues of the covariance matrix, $\lambda_1 > \lambda_2 > ... > \lambda_p$, are computed to be defined as the 'Feature A'. The eigenvalues are proportional to the (co)variance of the signal, and correspond to variance of principal components. Most of the information of (co)variance is therefore preserved by retaining a few biggest eigenvalues, $\lambda_1 > \lambda_2 > ... > \lambda_q$, $q \ll p$. It is expected that counterbore signals have lower variance and consequently lower eigenvalues. The classification can be performed based on the magnitude of calculated eigenvalues. The procedure for extracting the 'Feature A' is illustrated in Figure 4 (a).

Signal variances calculated from two hundred A-scans in each group, counterbore, rootweld and crack, are shown in Figure 5 (a). As expected, the variance of counterbore signals is much less than those of cracks and rootwelds. Dominant eigenvalues of covariance matrix of the three classes, crack, rootweld, and counterbore, are calculated and plotted in Figure 5 (b). These plots suggest that the dominant eigenvalues, obtained using a group of A-scans acquired from neighboring positions, offer a promising feature for classification.

Feature B: Variance of Principal Component

In order to calculate the 'Feature A', we need to calculate an estimate of the covariance matrix and eigenvalues for every set of unknown signals. This requires intensive computation when the dimension of signal is large.

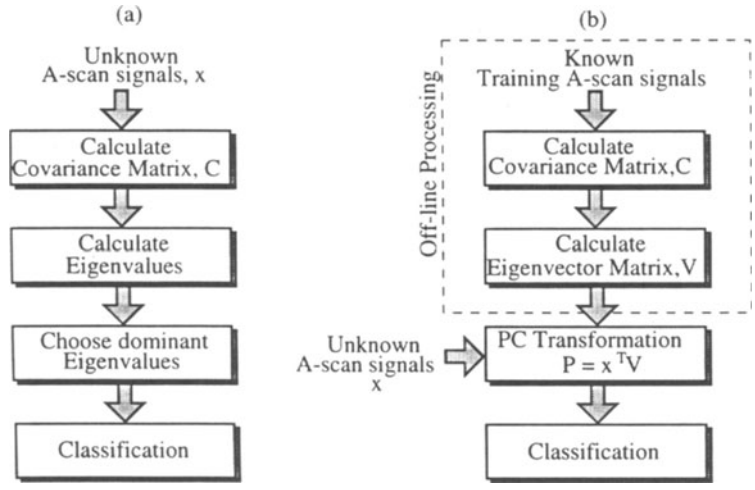

Figure 4: Feature extraction procedures for (a) 'Feature A' and (b) 'Feature B' given a set of unknown signals, $\vec{x}$.

In the case of the second feature, 'Feature B', the estimate of the covariance matrix and its eigenvector matrix are obtained *a priori* using known set of signals. First, an estimate of covariance matrix, $\hat{C}$ is calculated from a set of M known ultrasonic signals, $\vec{x}^m, m = 1, 2, ..., M$, of length p, where M is sufficiently large for obtaining an accurate estimate. Each element of the covariance matrix is then defined as

$$\hat{E}[x_i x_j] = \frac{1}{M}\sum_{n=1}^{M}(x_i^m - \frac{1}{M}\sum_{m=1}^{M} x_i^m)(x_j^m - \frac{1}{M}\sum_{m=1}^{M} x_j^m) \quad i,j = 1,2,...,p \tag{8}$$

The matrix, $V = [\vec{e}_1\ \vec{e}_2\ ...\ \vec{e}_q]$, consisting of its eigenvectors corresponding to $q(\ll p)$ largest eigenvalues is computed.

Given a set of N unknown signals, the principal component vector for each signal

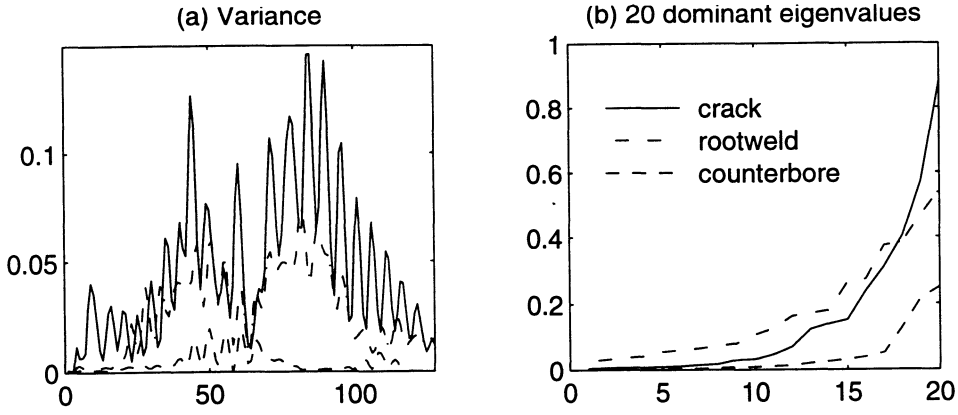

Figure 5: (a) Variance and (b) eigenvalues of the counterbore, rootweld and crack signals.

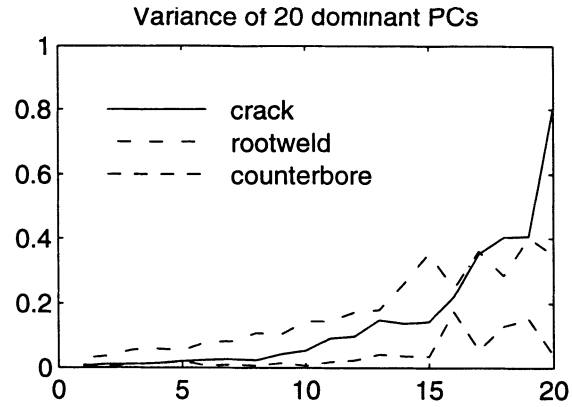

Figure 6: Variance of principal components of three signals: crack, counterbore and rootweld.

is calculated by the simple projection

$$(\vec{u}^n)^T = (\vec{x}^n)^T[\vec{e}_1\ \vec{e}_2\ ...\ \vec{e}_q],\ n = 1, 2, ..., N. \tag{9}$$

The 'Feature B' is defined as the variance of $\vec{u}^n$. The procedure for extracting the 'Feature B' is illustrated in Figure 4 (b).

This scheme provides a much faster way of extracting the measure of signal variation. in a reduced dimension, than the 'Feature A'. Figure 6 shows variance of 20 largest principal components calculated from the three classes. The covariance matrix is estimated from 200 signals from each class. The length or the dimension of signals, is 128, and it is reduced to 20 after projection. It is seen that the counterbore signals still shows the least variance in the reduced dimensional space of principal components.

CLASSIFICATION RESULTS AND DISCUSSIONS

The technique based on 'Feature A' and 'Feature B' was implemented on the C-scan images shown in Figure 2 and the classificaiton images are shown in Figure 7 and Figure 8, respectively. Each pixel of the processed images using 'Feature A' shown in Figure 7 corresponds to the biggest eigenvalue of the covariance matrix of 15 A-scans obtained from each 0.5"×0.075" area centered at the pixel in the C-scan image. In Figure 8 showing processed images using the 'Feature B', the variance of principal component is calculated from only the largest principal component. Classification images indicate only the crack regions. Rootweld and counterbore were correctly identified and eliminated in processed images.

Altough both features, 'A' and 'B', provide measures of signal variation in a reduced dimension, the extraction of the 'Feature B' requires much less processing time since the estimate of covariance matrix and its eigenvalues are not calculated for each set of unknown signals. A weighted combination of both features is currently being investigated for further optimization.

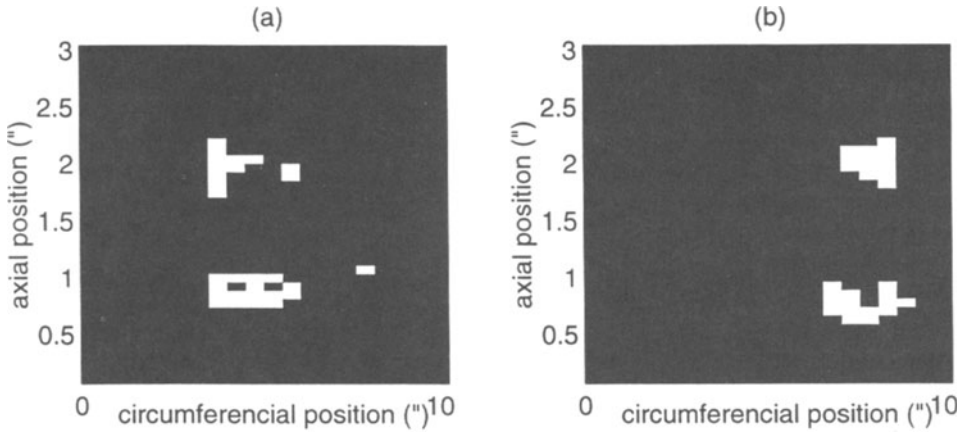

Figure 7: Classificaion images indicating regions of cracks using 'Feature A'. Rootwelds and counterbores are filtered out.

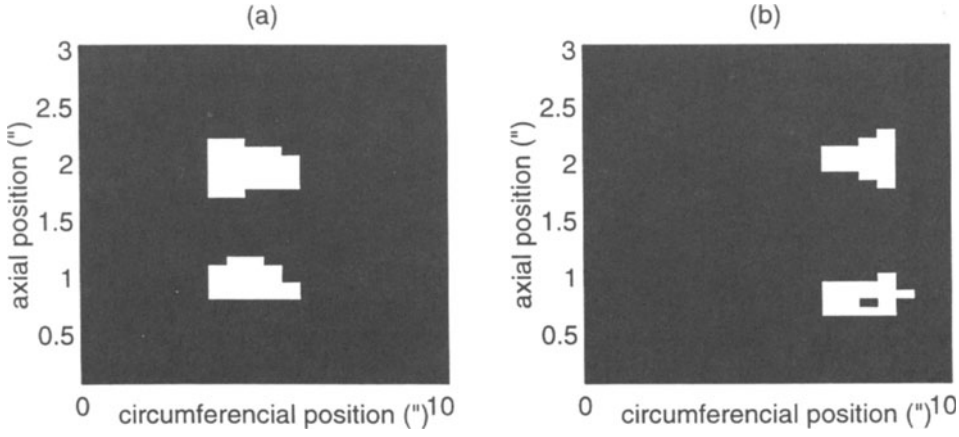

Figure 8: Classificaion images indicating regions of cracks using 'Feature B'. Rootwelds and counterbores are filtered out.

ACKNOWLEDGEMENTS

The study is sponsored by Electric Power Research Institute under contract RP3148-06.

REFERENCES

1. P. G. Heasler, T. T. Taylor, J. C. Spanner, S. R. Doctor, J. D. Deffenbaugh, Ultrasonic Inspection Reliability for Intergranular Stress Corrosion Cracking, May, 1990

2. Human Reliability in Inspection: Final Report on Action 7 in the PISC III Programme, PISC III report No. 31, February 2, 1994

3. S. F. Burch and N. K. Bealing, "A physical approach to the automated ultrasonic characterization of burried weld defects in ferrite steel", *NDT International*, Vol. 19, p. 145-153, 1986

4. A. R. Baker and C. G. Windsor, "The classification of defects from ultrasonic data using neural networks: The Hopfield method", *NDT International*, Vol. 22, p. 97-105, 1989
5. C. G. Windsor, F. Anselme, L. Capineri and J. P. Mason, "The classification of weld defects from ultrasonic images: a neural network approach", *The 31st Annual British Conference on NDT*, Cambridge, United Kingdom, Sep., 1992
6. I. T. Jolliffe, *Principal Component Analysis*, Springer-Verlag, New York, NY, 1986
7. S. Haykin, *Neural Networks: A Comprehensive Foundation* Macmillan Publishing Company, Englewood Cliffs, NJ, 1994
8. T. D. Sanger, "Optimal unsupervised learning in a single-layer linear feedforward neural network.", *Neural Networks*, Vol. 12, p. 459-473, 1989
9. J. Yang and G. A. Dumont, "Classification of acoustic emission signals via Hebbian feature extraction", *International Joint Conference on neural Networks*, Vol. 1, p. 113-118, Seattle, WA, 1991